SUPPLEMENTARY FIGURES AND TEXT

Figure S1. Ratios of SMARCAD1 binding on modified and unmodified histone peptides. Related to Figure 2A-B. Each row represents a histone peptide. The histone and amino acids (aa) are given at the top of the matrices. For example, H3 1-19 is the first 19 amino acids of histone 3. All columns except the last column represent the combination of post-translational modifications on this peptide. The last column represents the average ratio from two peptide arrays. In each array, the ratio is defined as the binding signal of the modified peptide divided by the binding signal of the unmodified peptide with identical aa sequence. The ratio is assigned as 1 (non-informative), if the binding signal on a modified peptide is not significantly larger than background. *: signal > 3-fold background in one array. **: signal > 3-fold background in both arrays.

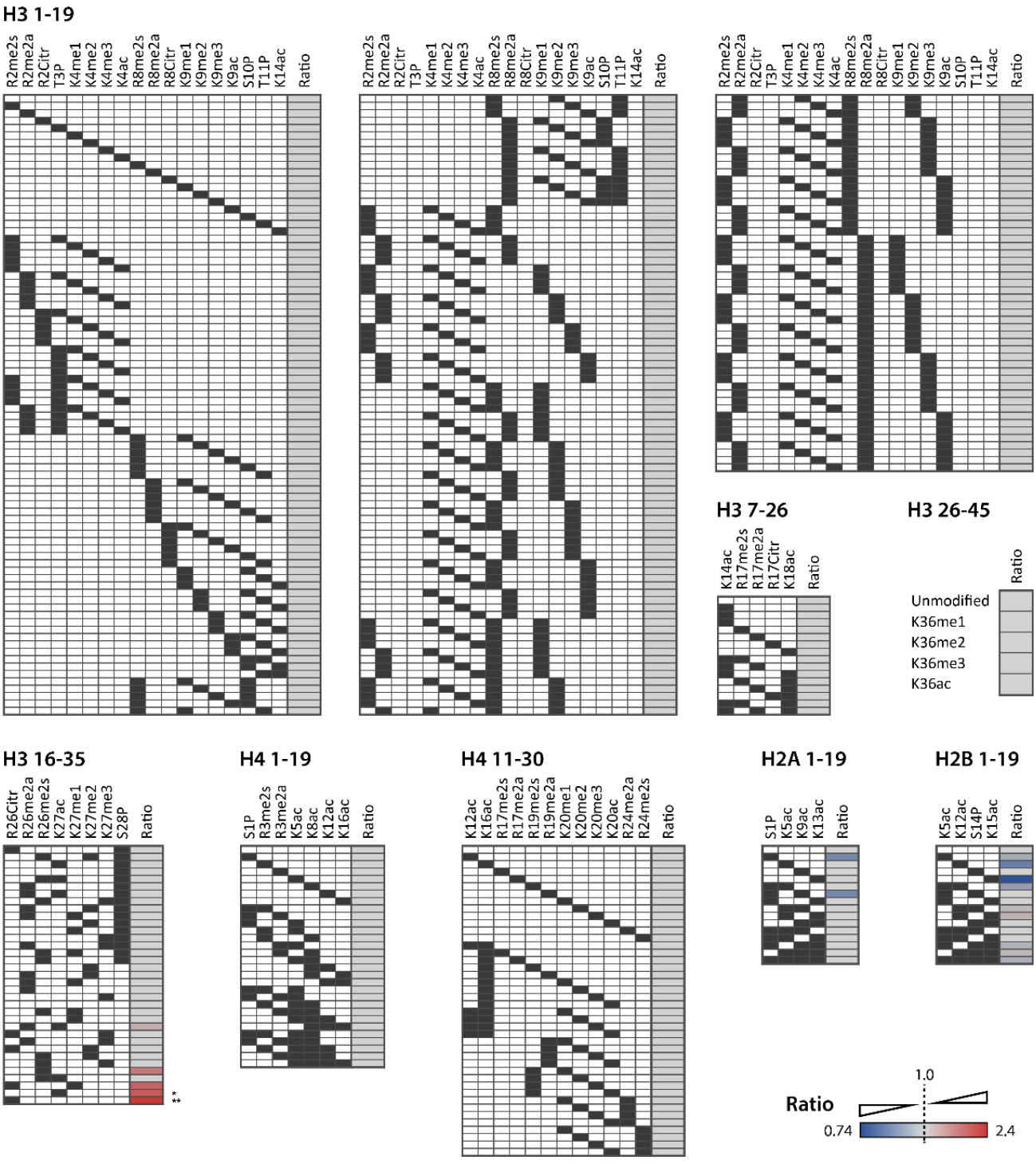

Figure S2. ChIP and western analyses. Related to Figure 2C-D and Figure 4F-G. (A) Degree of genome-wide co-localization between epigenetic modifications, measured as odds ratio (Xiao et al, 2012). Co-localizations that are larger, equal, and smaller than that from random permutation were plotted in red, white, and blue, respectively. (B) Size distributions of ChIP-seq peaks, called by MACS14 on E14 ES cell ChIP-seq data. (C) Cumulative overlap of the top ranked SMARCAD1 ChIP-seq peaks with H3K9me3 marked regions (red curve), as compared to that of SETDB1 and H3K9me3 (positive control, green), and NANOG and H3K9me3 (negative control, purple). (D) Venn diagram of SMARCAD1, SETDB1, and H3K9me3 peaks. (E) Distribution of distances between the centers of neighboring nucleosomes (y axis) in SMARCAD1 peaks (first column), H3R26Cit peaks occupied by SMARCAD1 (H3Cit-SMARCAD1), and the entire genome (third column). (F) Western blot showing the specificity of the SMARCAD1 antibody (Abcam, ab67548). Fluorescence is acquired from secondary antibodies, applied to SMARCAD1 primary antibody (green) and ladder (red). (G) Western blots of H3K9me2 and H3K9me3 in Luciferase KD (Control) and Smarcad1 KD (KD) cells. These are biological replicates to the data shown in Figure 4F-G.

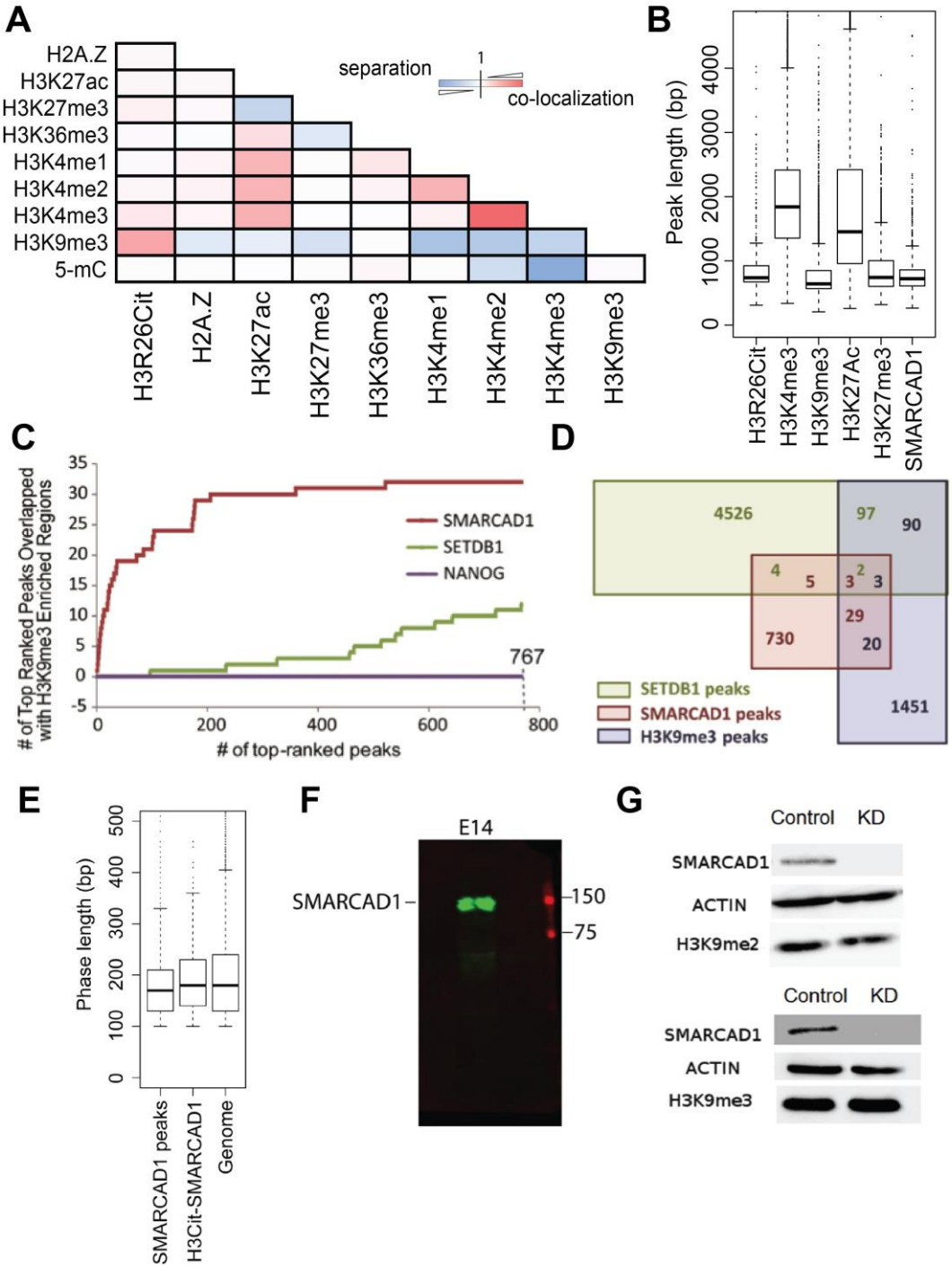

Figure S3. SMARCAD1 KD induced gene expression changes. Related to Figure 3. (A-C) Morphologies of control KD (Luci) and SMARCAD1 KD cells 35 passages after KD. Luci: a shRNA targeting Luciferase mRNA. RNAi1 – RNAi2: two shRNAs targeting different parts of Smarcad1 mRNA. (D) Fold changes of expression levels between Smarcad1 KD and control ES cells (y axis, in log scale). (E) Differentially expressed genes in the ACTIVIN/TGFβ signalling pathway. The magnitude of expression changes was represented by heatmap, and the direction of change was indicated by arrows. (F) Scatter plots of expression changes between EpiSC and ES cells (y axis) and expression changes between Smarcad1 KD and ES cells (x axis) in all the 13,599 detectable genes (FPKM > 0.1 in at least one dataset). (G) Venn diagram of genes with increase (log fold change > 1), decrease (log fold change < -1), or no change (-1 < log fold change < 1) of expression between Smarcad1 KD and ES (pink) and between EpiSC and ES (green). The total number of genes is 13,599, same as (A). P-value < 10^{-20}, Chi-squared test.

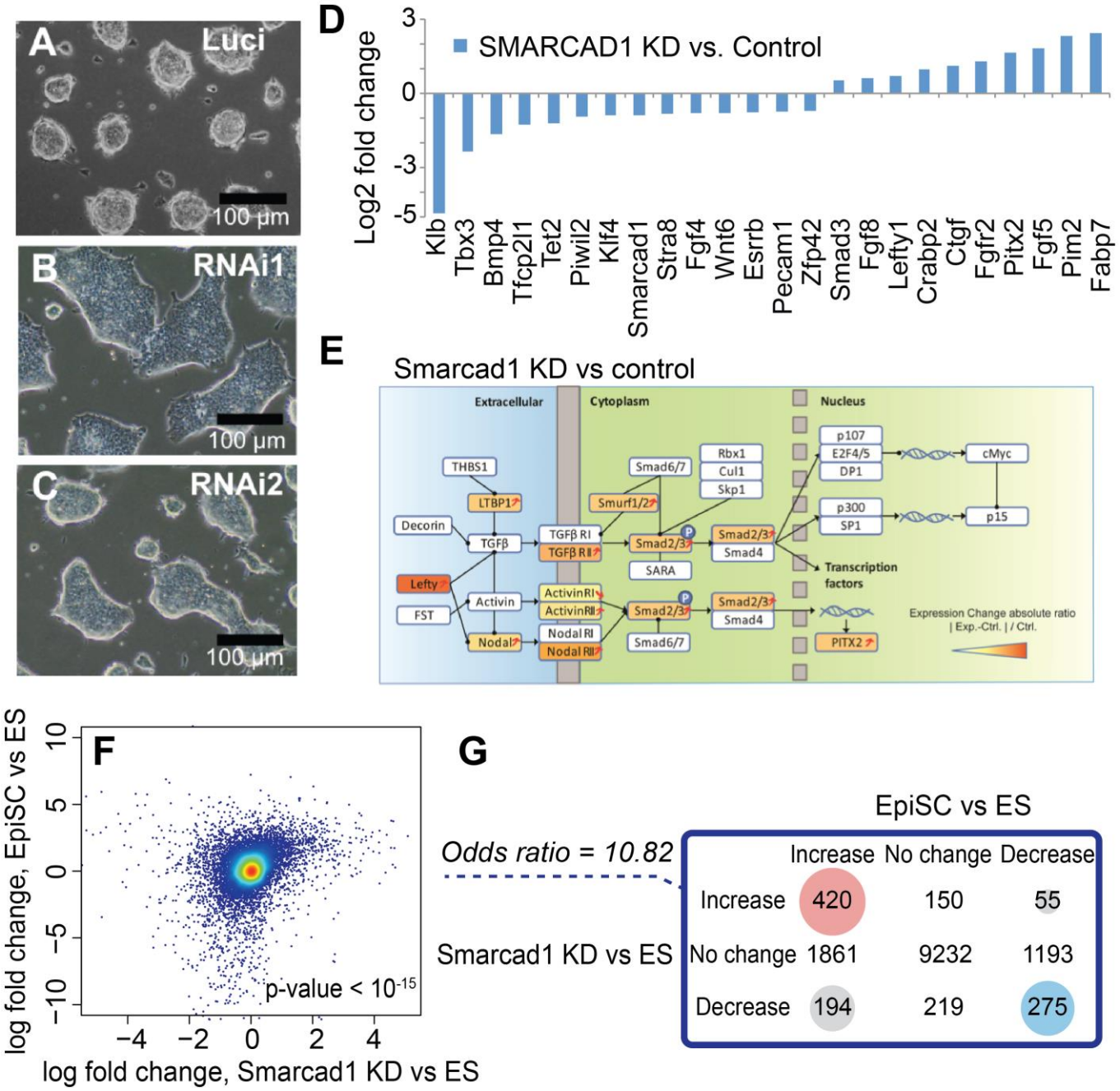

Figure S4. Changes in metabolism and pluripotent potential. Related to Figure 3. (A-B) Oxygen consumption rate (A), and extracellular acidification rate (B) normalized by total protein weight of the cells used for this experiment (y axis), measured at three time points (1.6, 8, 15 min) from the start (denoted as 0 min) of these measurements in control (Luciferase KD) ES (Control, left columns) and Smarcad1 KD (right columns) ES cells. Error bar: standard deviation of the mean from 3 biological replicates. (C-E) ICM integration of Smarcad1 KD ES cells. (C) qPCR analysis of Luciferase KD (control, blue) and Smarcad1 KD Ogr1 ES cells (orange). Error bars: standard deviation derived from three biological replicates. Representative images of Ogr1 ES (D) and Smarcad1 KD Ogr1 ES cell (E) integration into ICM. Scale bar = 50 µm.

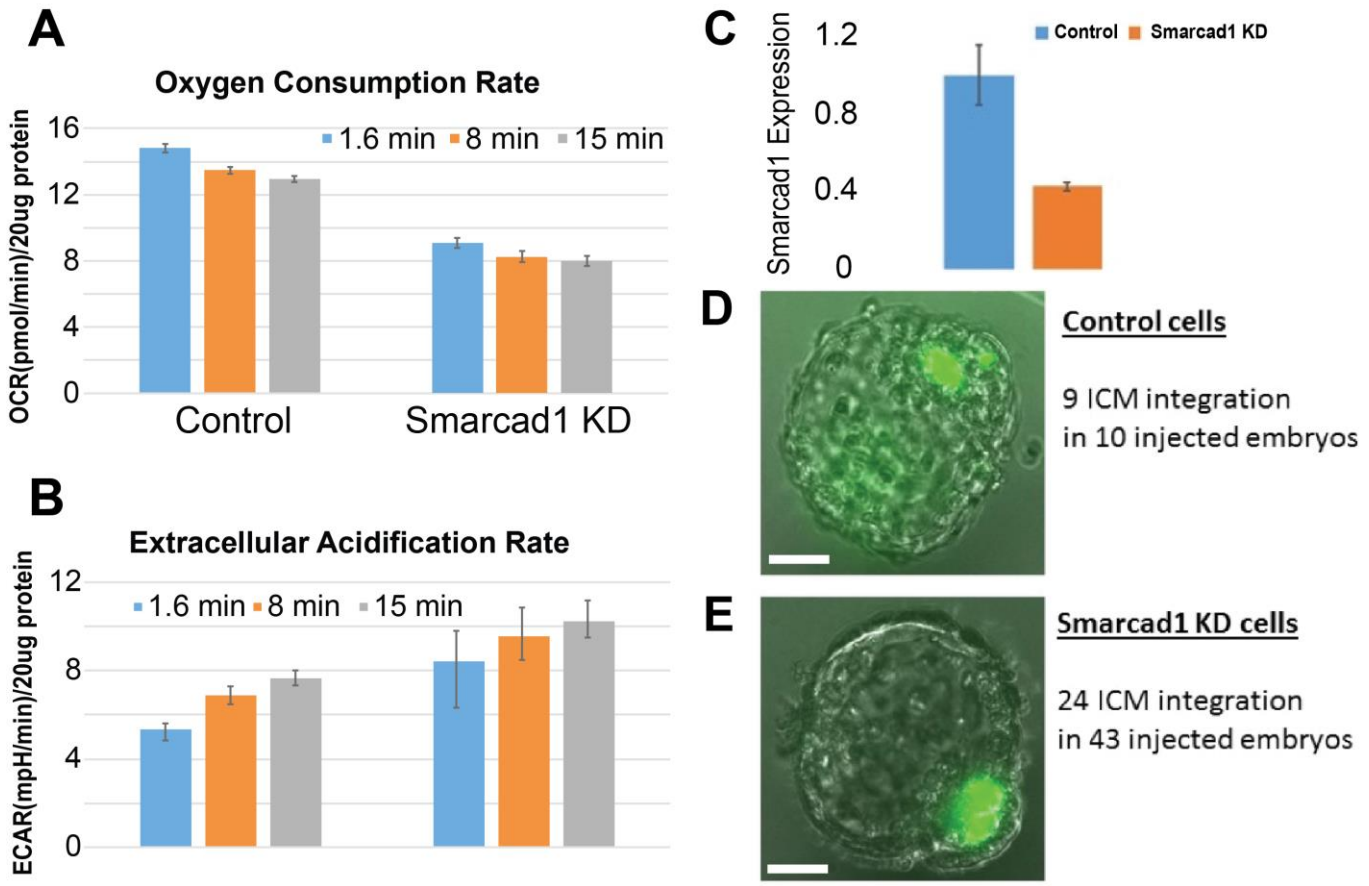

Figure S5. Invariant features between Smarcad1 KD and control cells. Related to Figure 3. (A) Expression levels of two senescence marker genes in Control (Luciferase KD, green) and Smarcad1 KD cells (yellow). Error bars were derived from two biological replicates. (B-C) Cell proliferation curves. Smarcad1 KD and Control (Luciferase KD) cells were seeded with 83,000 cells per well (B) and 42,000 cells per well (C), and subsequently quantified (y axis) at 24, 48, and 72 hours (x axis). (D-E) Embryoid bodies (EBs) derived from Control (Luciferase KD) and Smarcad1 KD cells. (F) RT-PCR derived expression fold changes (EB / ES) of lineage markers, in control EBs (green) and Smarcad1 KD cell derived EBs (yellow). E14: mouse ES cells. (G-H) Teratomas originated from Smarcad1 KD cells (G) and Luciferase KD cells (H).

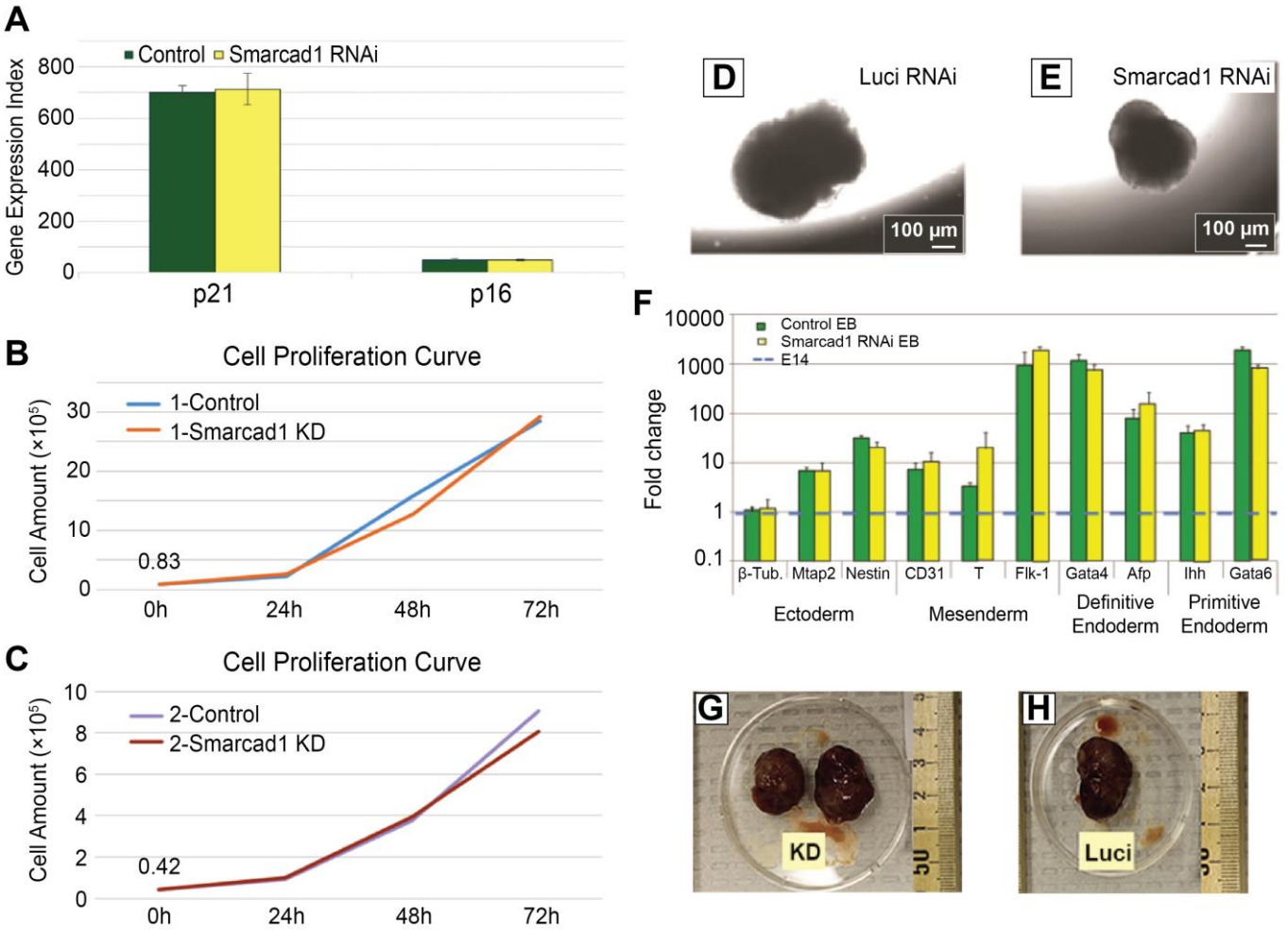

Figure S6. Smarcad1 KD mediated changes in SMARCAD1 binding and H3K9me3 deposition. Related to Figure 4. (A-D) Gene expression level (bar plots), SMARCAD1 occupancy (SMARCAD1 track), H3K9me3 in ES cells (H3K9me3 track) and in Smarcad1 KD (H3K9me3 Smarcad1 KD track) levels near Klf4 (A), Wnt6 (B), and Fgfr4 (C) and Paqr6 (D). (E) Association between SMARCAD1 peaks and major classes of genomic repeats (x axis). Odds ratio (y axis, in log scale) was used to quantify the association, comparing the fraction of SMARCAD1 peaks that contain a class of repeats to the genome. A positive log odds ratio suggests enrichment. (F) Association of Smarcad1 KD induced H3K9me3 peaks with genomic repeats and other genomic features (x axis). A positive log odds ratio (y axis) suggests an enrichment of H3K9me3 changes in this class of repeats.

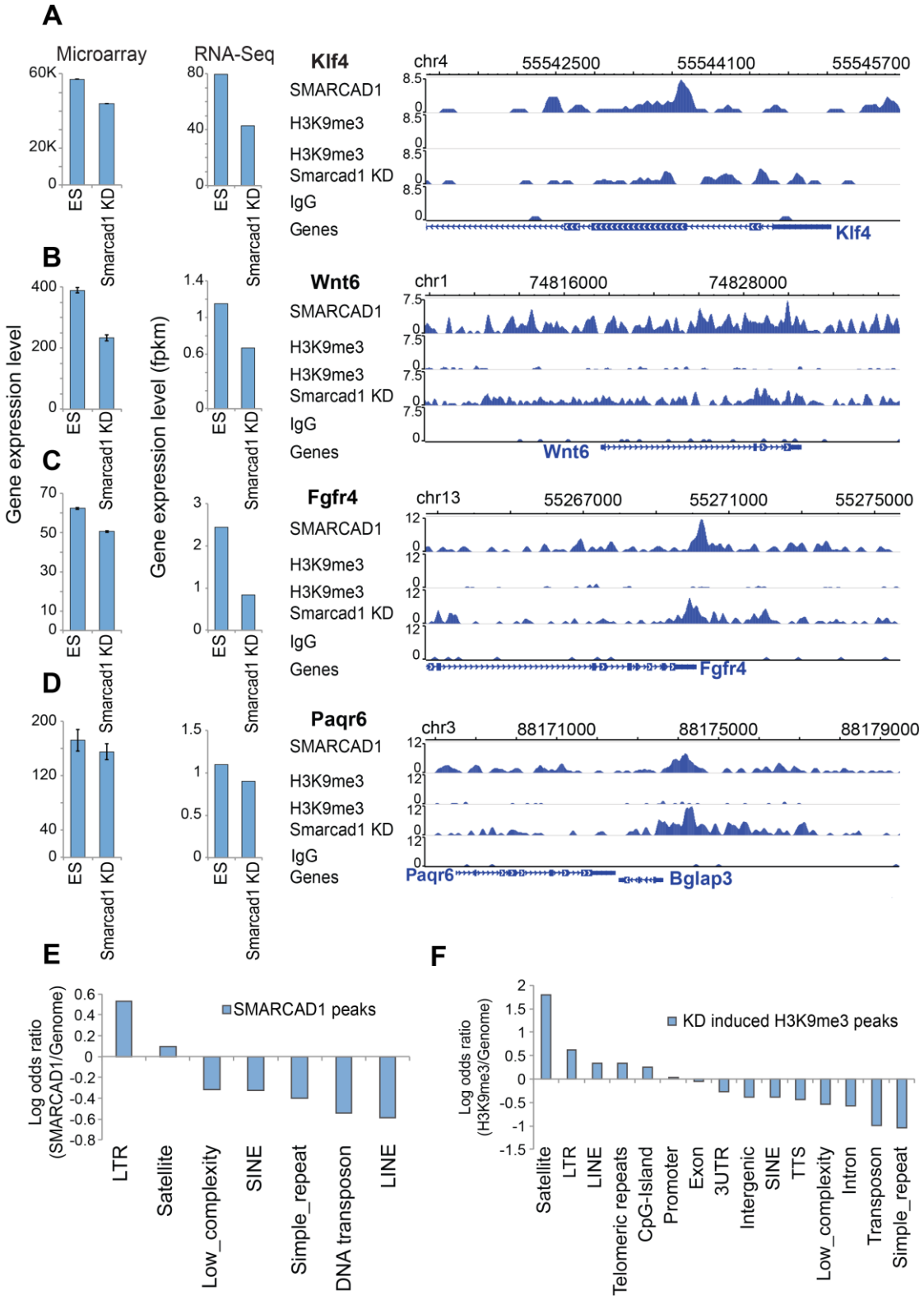

SUPPLEMENTARY TABLES

Table S1. Summary of teratomas. Related to Figure 3. The teratomas originating from control knockdown cells (Control column) and from SMARCAD1 knockdown (KD column). L, R: the side of the body. Y: tumor found at this site. N: no tumor found.

Mouse	Injection	Control	KD
1	L (Control), R	Y (L)	Y (R)
1	L (Control), R	Y (L)	Y (R)
2	L, R (Control)	Y (R)	Y (L)
2	L, R (Control)	Y (R)	N
3	L (Control), R	Y (L)	Y (R)
3	L (Control), R	Y (L)	Y (R)
4	L, R (Control)	Y (R)	Y (L)
4	L, R (Control)	N	Y (L)

Table S2. Primer sequences used in RT-PCR analysis. Related to Figure 3.

Gene	Forward primer	Reverse primer
Actin	AGGCTCTTTTCCAGCCTTCCT	GTCTTTACGGATGTCAACGTCACA
Oct4	CTGGGGGTTCTCTTTGGAAA	TATCTCCTGAAGGTTCTCATTGTTGT
Nanog	AGCCTCCAGCAGATGCAAGA	TGCACCGCTTGCACTT
Sox2	AACTTTTGTCCGAGACCGAGAA	CCGCGGCCGGTATTTATAAT
Smarcad1	TGAATTTTGTTATGCCACACATGTT	CTCTGCTCGTCTGCTGGTTTC
β-Tubulin	TGGAGCGCATCAGCGTAT	CGCCAGACCGAACACTG
CD31	TGCACAGTGATGCTGAACAA	CGCCTTCTGTCACCTCCT
Gata4	ATCGCGCCGGTTTTCT	CTCCAGAGCGGCTCCA
Gata6	GAGGGTGAGCCTGTGTGC	GGTTTTCGTTTCCTGGTTTG
Mtap2	ACCTTCGCCACCACCAT	CGCCTGTTTAAAAGCACCA
Brachyury	CGCCTGTGTCTTTCAGCA	CCCCCAACTCTCACGATG
Flk-1	TTGGCAAATACAACCCTTCA	TCACCAATACCCTTTCCTCA
Afp	ATTTCTCGGGCCTTTTGG	GCCCAAAGCATCACGAGT
Ihh	CGGCTTCGACTGGGTGTA	CTCCGGCAGGAAAGCAG
Nestin	GCAACTGGCACACCTCAA	CCAAGAGAAGCCTGGGAAC

SUPPLEMENTARY ANALYSIS

Comparison of gene expression data

Our microarrays and Tesar's microarrays (Tesar et al., 2007) were from different manufacturers, which were not expected to reproduce the detected differentially expressed genes (Fortunel et al., 2003). However, the microarray detected differentially expressed genes between Smarcad1 KD and ES cells were correlated with that between primed and naïve pluripotent cells (Tesar et al., 2007) (p-value = 5×10^{-8}, Chi-square test). We compared our RNA-seq data with published RNA-seq data in EpiSC and ES cells (GSE57403) (Factor et al., 2014). Based on all the genes (13,599) with detectable expression (FPKM ≥ 0.1) in least one RNA-seq dataset, the genomewide expression changes between Smarcad1 KD and ES cells exhibited a weak correlation with the genomewide changes between EpiSC and ES cells (p-value < 10^{-15}, T test) (Figure S3F). Next, we identified and compared the differentially expressed genes (1,313) between Smarcad1 KD and control ES cells (log fold change > 1 or <-1) with the differentially expressed genes (3,998) between EpiSC and ES cells (log fold change > 1 or <-1). The up- or down-regulated genes in Smarcad1 KD were associated with that in EpiSC (odds ratio = 10.8, p-value < 10^{-20}, Chi-squared test, Figure S3G).

Potential association of retrotransposons and satellite repeats with Smarcad1 KD mediated H3K9me3 changes

It remains unresolved whether any genomic features are associated with SMARCAD1 accessed genomic loci. Our de novo motif search did not identify significant sequence motifs in SMARCAD1 peaks. However, more LTR retrotransposons and satellites appeared in SMARCAD1 peaks than expected from the genome average (Figure S6F). Considering that our HT-SELEX experiment failed to identify SMARCAD1 binding to specific DNA sequences *in vitro*, this enrichment may reflect binding preferences of co-factors rather than that of SMARCAD1 itself.

Next, we examined genomic features associated with Smarcad1 KD induced H3K9me3 peaks. We considered 7 types of DNA repeats and other genomic features including CpG islands, intragenic regions, promoters, exons, introns, and 3' untranslated regions. Smarcad1 KD induced H3K9me3 peaks were enriched in satellites and LTR retrotransposons, as compared to the genome background (Fisher's Exact Test p-value < 10^{-8}) (Figure S6G). Interestingly, although this analysis was independent of SMARCAD1 ChIP-seq data, it prioritized the same genomic features as that enriched in SMARCAD1 peaks.

SUPPLEMENTARY METHODS

Immunosurgery of mouse blastocysts

Mouse ICMs were surgically isolated from 3.5 day blastocysts by cutting off the zona pellucida and tearing off the trophoblastic layer from the nudity blastocyst as previously described (Sviridova-Chailakhyan et al., 2008).

RNA-seq experiment

RNA extraction and amplification from preimplantation embryos and ICM were carried out as described before (Xie et al., 2010). The amplified RNAs were subjected to sequencing using Illumina's small sample RNA-seq protocol.

Cell culture

Mouse E14, Ogr1 (Chowdhury et al., 2010) ES cells and SMARCAD1 KD ES cells were cultured under feeder-free condition with LIF supplementation as previously described (Li et al., 2011). EpiSCs were a gift from Azim Surani (Bao et al., 2009). Switch to EpiSC culture medium was described in Methods of the main text. Pig naïve ES cells and primed iPS cells were maintained as previously described (Ezashi et al., 2009; Telugu et al., 2011).

Western blot

Proteins were separated from homogenized cells, transferred onto nitrocellulose membrane (Amersham), and probed with antibodies. The antibodies were SMACARD1 (Abcam, ab67548), H3R26Cit (Abcam, ab19847), H3K9me3 (Abcam, ab8898), H3K9me2 (Abcam, ab1220), ACTIN (Abcam, ab3280), α-TUBLIN (Abcam, ab11304), OCT4 (Santa Cruz, SC-9081), SOX2 (Millipore, ab5603), NANOG (Cell Signaling, 3580). The vendor's website has western blots showing the specificity of these antibodies. The H3R26Cit antibody was used in Zhang et al., PNAS 2012 (Zhang et al., 2012). The other protein and histone antibodies were used a number of previous publications including Xiao et al., Cell 2012 (Xiao et al., 2012).

RNA knockdown

Two shRNAs targeting different parts of the mouse Smarcad1 mRNA were constructed by cloning oligos into pSUPER.puro (BglII and HindIII sites, Oligoengine) (Hong et al., 2009). The shRNA sequences were: GAAGAGCGTAAGCAAATTA, GTATGAGGATTACAATGTA. Both pSUPER.puro and a pSUPER.puro loaded with a shRNA targeting Firefly Luciferase mRNA (pSuper-Luci) were used as controls. Cells were transfected with shRNA constructs by Lipofectamine 2000 (Invitrogen) followed by Puromycin (Sigma) selection. The ES cells were digested with dispase and subcultured 5 days after shRNA transfection. Cell images and western blots were generated 10 days after transfection. All procedures were repeated with identical procedures except one step, in which trypsin-EDTA was used for digestion on the 5^{th} day.

Alkaline Phosphatase (AP) staining

An AP detection kit (Millipore) was used for AP staining. Images were taken from an AMG EVOS XL microscope.

Xist expression

Female mouse ES cells EL16.6 (Zhao et al., 2008) were transfected with shRNAs against Smarcad1 and Luciferase and puromycin selected. Xist qPCR were carried out as previously described, using Xist specific probes that cannot amplify Tsix (Zhao et al., 2008).

Chimera analysis

Ogr1 ES cells were used for chimera analysis, as previously described (Li et al., 2011)**.** Ogr1 ES cells "contain an Oct4-GFP transgenic reporter under the control of the entire 18Kb Oct4 regulatory sequences" (Yeom et al., 1996). We injected Smarcad1 KD Ogr1 and Ogr1 cells into 3.5 day embryos (C57/BL6) and checked for chimera formation in approximately the next 28 – 32 hours.

Teratoma generation and histological analysis

Cells were collected by triple digestion, re-suspended in PBS ($2x10^6$ cells / 25uL of PBS), mixed with collagen (0.3mg/mL), and injected into 4 female mice. Each mouse received 4 subcutaneous injections with 2 injections per flank. Teratomas were collected 28 days after injections and fixed with 4% paraformaldehyde. Two of the four mice developed an equal number of teratomas from Smarcad1 KD cells and from control cells (Mice 1 and 3 in Table S1). The other two mice developed unbalanced number of teratomas: one had two tumors from Smarcad1 KD cells and one tumor from control cells, and the other had a reversed scenario (Mice 2 and 4 in Table S1). Slices of the fixed teratomas were stained with Hematoxylin and Eosin, and imaged with a NanoZoomer Digital Pathology System (Hamamatsu).

Quantification of metabolic features

Oxygen consumption rate (OCR) and extracellular acidification rate (ECAR) were quantified as previously described (Zhou et al., 2012). Briefly, approximately 150,000 control (Luciferase KD) and Smarcad1 KD cells in confluence are subjected to measurement by a Seahorse XF Analyzer (Agilent), at three time points (1, 8, and 15 minutes). Culture medium was changed into a base medium (unbuffered DMEM (Sigma D5030) supplemented with 2 mM Glutamine) 1 hour before the assay. Three biological replicates were measured. After the assay, cells were lysed and protein weight was measured by NanoDrop™ 1000 Spectrophotometer. The protein weights were used to normalize OCR and ECAR.

RT-PCR

Total RNA was extracted, and first-strand cDNA was synthesized with an M-MLV Synthesis System (New England Biolabs) and subsequently analyzed with an Applied Biosystems 7900HT Fast Real-Time PCR System. Primer sequences are listed in Table S2. β-actin was used as the internal control to normalize cycle numbers.

Embryoid body (EB) formation

Clusters of 200 cells were suspended in 30 µL of stem cell media without LIF. These droplets were hung on a petri dish cap for 3 days, and then collected and maintained with mild shaking in a 37 C incubator for 14 days. EB images were taken on the 14th day of incubation.

Gene Expression Microarray

Total RNA was isolated with Trizol (Invitrogen), labeled, and hybridized onto Agilent-014868 Whole Mouse Genome Microarray 4x44K G4122F.

ChIP-Seq and data analysis

ChIP-Seq was carried out as previously described (Xiao et al., 2012) with E14 ES cells, Smarcad1 KD E14 ES cells, and Cl-Amidine treated E14 cells. The antibodies were SMARCAD1 (Abcam, ab67548), H3R26Cit

(Abcam, ab19847), H3K9me3 (Abcam, ab8898), H3K27Ac (Abcam, ab4729), H3K4me3 (ab8580). For Wu1 ES cells (Wu et al., 2015), we transferred Wu1 cells from 2i medium to the ES culture condition (Li et al., 2011) for 48 hours, and then performed SMARCAD1 ChIP-seq. ChIP-seq data were aligned to the mouse (mm9) genome using Bowtie software with unique alignment and ≤ 1 mismatch (Langmead et al., 2009). MACS (version 1.4.0beta) was used to call ChIP-seq peaks with default parameters and IgG ChIP-seq as control (Feng et al., 2012). In addition, input DNA were sequenced as follows. We fragmented E14 chromatin by MNase and sequenced to yield 120,978,017 mappable single-end 100 nt reads, which corresponds to approximately 6 fold genome coverage. We note that all ChIP-seq peaks were called using IgG, not input DNA, as control.

Analysis of RNA-seq data

RNA-seq data were aligned to mouse (mm9) genome using Tophat with unique alignment and ≤ 1 mismatch (Trapnell et al., 2009). Cufflinks with default parameters was used to estimate the expression levels (Trapnell et al., 2012).

Analysis of nucleosome phase length

E14 ES cell MNase-seq data (Teif et al., 2014) were downloaded from GEO (GSE56938) and aligned to mouse genome (mm9) with Bowtie2 (v2.2.6). The reads with MAPQ ≥ 2 were retained, and nucleosome positions were called by DANPOS (v2.2.2) (Chen et al., 2013). When calculating the distances between nucleosome centers in SMARCAD1 peaks and in H3R26Cit peaks, these peaks were extended by 200 bp on each end, so that each peak covers at least two nucleosomes.

REFERENCES TO SUPPLEMENTARY TEXT

Bao, S., Tang, F., Li, X., Hayashi, K., Gillich, A., Lao, K., and Surani, M.A. (2009). Epigenetic reversion of post-implantation epiblast to pluripotent embryonic stem cells. Nature *461*, 1292-1295.

Chen, K., Xi, Y., Pan, X., Li, Z., Kaestner, K., Tyler, J., Dent, S., He, X., and Li, W. (2013). DANPOS: dynamic analysis of nucleosome position and occupancy by sequencing. Genome research *23*, 341-351.

Chowdhury, F., Li, Y., Poh, Y.-C., Yokohama-Tamaki, T., Wang, N., and Tanaka, T.S. (2010). Soft Substrates Promote Homogeneous Self-Renewal of Embryonic Stem Cells via Downregulating Cell-Matrix Tractions. PLoS ONE *5*, e15655.

Ezashi, T., Telugu, B.P., Alexenko, A.P., Sachdev, S., Sinha, S., and Roberts, R.M. (2009). Derivation of induced pluripotent stem cells from pig somatic cells. Proceedings of the National Academy of Sciences of the United States of America *106*, 10993-10998.

Factor, D.C., Corradin, O., Zentner, G.E., Saiakhova, A., Song, L., Chenoweth, J.G., McKay, R.D., Crawford, G.E., Scacheri, P.C., and Tesar, P.J. (2014). Epigenomic comparison reveals activation of "seed" enhancers during transition from naive to primed pluripotency. Cell Stem Cell *14*, 854-863.

Feng, J., Liu, T., Qin, B., Zhang, Y., and Liu, X.S. (2012). Identifying ChIP-seq enrichment using MACS. Nature protocols *7*, 1728-1740.

Fortunel, N.O., Otu, H.H., Ng, H.H., Chen, J., Mu, X., Chevassut, T., Li, X., Joseph, M., Bailey, C., Hatzfeld, J.A*., et al.* (2003). Comment on " 'Stemness': transcriptional profiling of embryonic and adult stem cells" and "a stem cell molecular signature". Science *302*, 393; author reply 393.

Hong, F., Fang, F., He, X., Cao, X., Chipperfield, H., Xie, D., Wong, W.H., Ng, H.H., and Zhong, S. (2009). Dissecting early differentially expressed genes in a mixture of differentiating embryonic stem cells. PLoS computational biology *5*, e1000607.

Langmead, B., Trapnell, C., Pop, M., and Salzberg, S.L. (2009). Ultrafast and memory-efficient alignment of short DNA sequences to the human genome. Genome Biol *10*.
Li, Y., Yokohama-Tamaki, T., and Tanaka, T.S. (2011). Short-term serum-free culture reveals that inhibition of Gsk3beta induces the tumor-like growth of mouse embryonic stem cells. PloS one *6*, e21355.
Sviridova-Chailakhyan, T.A., Tzoy, N.G., Panchenko, M.M., Akatov, V.S., and Chailakhyan, L.M. (2008). An efficient method for isolation of inner cell masses from the mouse blastocysts for culturing embryonic stem cells. Doklady biological sciences : proceedings of the Academy of Sciences of the USSR, Biological sciences sections / translated from Russian *423*, 469-472.
Teif, V.B., Beshnova, D.A., Vainshtein, Y., Marth, C., Mallm, J.P., Hofer, T., and Rippe, K. (2014). Nucleosome repositioning links DNA (de)methylation and differential CTCF binding during stem cell development. Genome research *24*, 1285-1295.
Telugu, B.P., Ezashi, T., Sinha, S., Alexenko, A.P., Spate, L., Prather, R.S., and Roberts, R.M. (2011). Leukemia inhibitory factor (LIF)-dependent, pluripotent stem cells established from inner cell mass of porcine embryos. The Journal of biological chemistry *286*, 28948-28953.
Tesar, P.J., Chenoweth, J.G., Brook, F.A., Davies, T.J., Evans, E.P., Mack, D.L., Gardner, R.L., and McKay, R.D. (2007). New cell lines from mouse epiblast share defining features with human embryonic stem cells. Nature *448*, 196-199.
Trapnell, C., Pachter, L., and Salzberg, S.L. (2009). TopHat: discovering splice junctions with RNA-Seq. Bioinformatics *25*, 1105-1111.
Trapnell, C., Roberts, A., Goff, L., Pertea, G., Kim, D., Kelley, D.R., Pimentel, H., Salzberg, S.L., Rinn, J.L., and Pachter, L. (2012). Differential gene and transcript expression analysis of RNA-seq experiments with TopHat and Cufflinks. Nat Protoc *7*, 562-578.
Wu, J., Okamura, D., Li, M., Suzuki, K., Luo, C., Ma, L., He, Y., Li, Z., Benner, C., Tamura, I.*, et al.* (2015). An alternative pluripotent state confers interspecies chimaeric competency. Nature *521*, 316-321.
Xiao, S., Xie, D., Cao, X., Yu, P., Xing, X., Chen, C.C., Musselman, M., Xie, M., West, F.D., Lewin, H.A.*, et al.* (2012). Comparative epigenomic annotation of regulatory DNA. Cell *149*, 1381-1392.
Xie, D., Chen, C.C., Ptaszek, L.M., Xiao, S., Cao, X., Fang, F., Ng, H.H., Lewin, H.A., Cowan, C., and Zhong, S. (2010). Rewirable gene regulatory networks in the preimplantation embryonic development of three mammalian species. Genome research *20*, 804-815.
Yeom, Y.I., Fuhrmann, G., Ovitt, C.E., Brehm, A., Ohbo, K., Gross, M., Hubner, K., and Scholer, H.R. (1996). Germline regulatory element of Oct-4 specific for the totipotent cycle of embryonal cells. Development *122*, 881-894.
Zhang, X., Bolt, M., Guertin, M.J., Chen, W., Zhang, S., Cherrington, B.D., Slade, D.J., Dreyton, C.J., Subramanian, V., Bicker, K.L.*, et al.* (2012). Peptidylarginine deiminase 2-catalyzed histone H3 arginine 26 citrullination facilitates estrogen receptor alpha target gene activation. Proceedings of the National Academy of Sciences of the United States of America *109*, 13331-13336.
Zhao, J., Sun, B.K., Erwin, J.A., Song, J.J., and Lee, J.T. (2008). Polycomb proteins targeted by a short repeat RNA to the mouse X chromosome. Science *322*, 750-756.
Zhou, W., Choi, M., Margineantu, D., Margaretha, L., Hesson, J., Cavanaugh, C., Blau, C.A., Horwitz, M.S., Hockenbery, D., Ware, C.*, et al.* (2012). HIF1alpha induced switch from bivalent to exclusively glycolytic metabolism during ESC-to-EpiSC/hESC transition. EMBO J *31*, 2103-2116.